ISSN (Print) 1226-1750
ISSN (Online) 2233-6656
Journal of Magnetics 18(3), 297-301 (2013) http://dx.doi.org/10.4283/JMAG.2013.18.3.297

A Study on the Iron Loss and Demagnetization Characteristics of an Inset-type Flux-Reversal Machine

Tae Heoung Kim*

Department of Electrical Engineering, Engineering Research Institute, Gyeongsang National University, Gyeongnam 660-701, Korea

(Received 27 May 2013, Received in final form 10 July 2013, Accepted 15 July 2013)

Flux-reversal machine (FRM) is cost effective and suitable for mass production due to its simple structure. However, there is a notable permanent magnet flux leakage which deteriorates the performance. To compensate this drawback with a design method, an Inset-Permanent-Magnet-Type FRM (ITFRM) has been proposed. The ITFRM has permanent magnets perpendicular to the stator teeth surface, and thus, is much more difficult to demagnetize. In this paper, we deal with the iron losses and irreversible permanent magnet demagnetization characteristics of the ITFRM according to various design variables and driving conditions. To analyze the characteristics, a two-dimensional finite-element method (2D-FEM) considering nonlinear analysis of permanent magnets is used. As a result, we propose the design variables that have the largest effects on the iron losses and irreversible magnet demagnetization.

Keywords : flux-reversal machine, iron loss, permanent magnet

1. Introduction

In spite of having permanent magnets on the stator to produce a magnetic torque, the flux linkage in the stator phase concentrated coils of a flux-reversal machine (FRM) reverses polarity with the rotor traveling. It also has a low self and mutual inductance, a low electrical time constant and high fault tolerance [1-4]. Thus, it is suitable for mass production and variable speed applications such as home appliances. However, there are considerable permanent magnet flux leakage, cogging torque and irreversible permanent magnet demagnetization problems due to its inherent structure. This flux leakage deteriorates the power density and torque ability of the FRM. The cogging torque also produces an additional acoustic noise [5]. Specifically, for home appliances which need high-reliability, it is very important to predict the irreversible demagnetization and design such machine to avoid the issue. To compensate for this weakness with a design method and to improve the performance of the FRM, a new inset-permanent-magnet-type FRM (ITFRM) has been proposed [6]. This ITFRM has permanent magnets perpendicular to the stator teeth surface, and thus, is much more difficult to demagnetize.

*Corresponding author: Tel: +82-55-772-1717
Fax: +82-55-772-1719, e-mail: ktheoung@gnu.ac.kr

In this paper, we analyze the effects of various design variables and magnet shapes for the iron losses and irreversible magnet demagnetization characteristics of the ITFRM. The iron losses consist of hysteresis and eddy current loss, which were calculated from the time variation of the magnetic field distribution that is obtained by a two-dimensional finite-element method (2D-FEM). We also used nonlinear analysis of the permanent magnet to estimate the magnet demagnetization. As a result, we investigate and propose the design variables that acquire the largest effects on the iron losses and irreversible magnet demagnetization.

2. Analysis Model and Basic Characteristics

Fig. 1 shows the structure of the inset-type FRM, as compared to a conventional one. It has a six-pole stator and eight-pole variable reluctance rotor. The permanent magnet is sintered Nd-Fe-B with 2 mm thickness. The 0.5 mm mechanical air-gap has been chosen to obtain a reasonable permeance coefficient. The constructed prototype FRM and the important FRM design specifications are shown in Fig. 2 and Table 1, respectively. Fig. 3 shows the back electro-motive force (BEMF) at 1500 rpm. It has some harmonics due to saturations of the magnetic circuit. Therefore, we need to decrease the harmonics to improve performances. Fig. 4 illustrates a self-inductance waveform. We can observe the inductance variation with the rotor

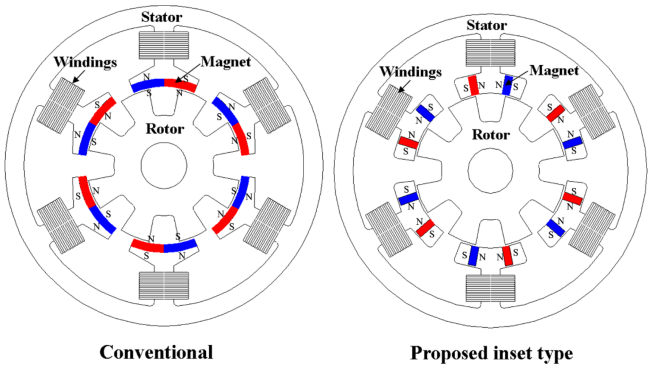

Fig. 1. (Color online) The conventional and inset-type FRM.

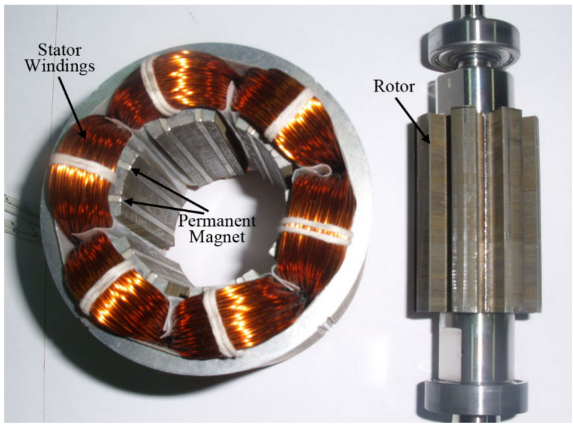

Fig. 2. (Color online) The constructed prototype FRM.

Table 1. Specifications of the inset-type FRM.

Section	Item	Value	(Unit)
	Number of phases	3	
	Number of slots	6	
Stator	Outer diameter	83	(mm)
	Stack width	60	(mm)
	Number of turns / phase / pole	196	(turns)
	Number of poles	8	
Rotor	Outer diameter	40	(mm)
	Pole length	7.85	(mm)
	Power	100	(W)
Rated	Speed	1500	(rpm)
	Voltage	110	(Vrms)
Air gap	Mechanical air gap	0.5	(mm)

rotating. The conventional FRM have no inductance variation due to a large electrical air-gap between the stator and rotor. However, the ITFRM has a little variation, which can be used to produce an additional reluctance torque. Thus, the torque ability is more excellent than that of the conventional FRM.

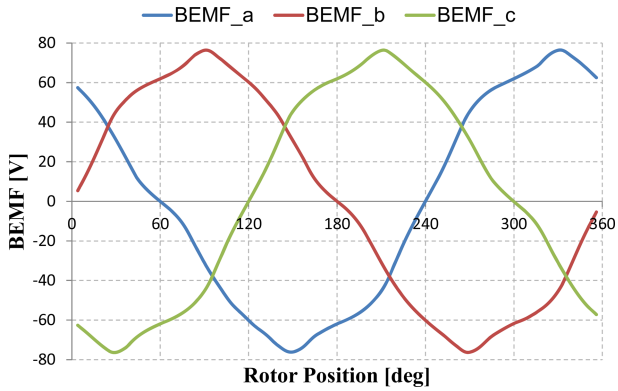

Fig. 3. (Color online) BEMF waveform at 1500 rpm.

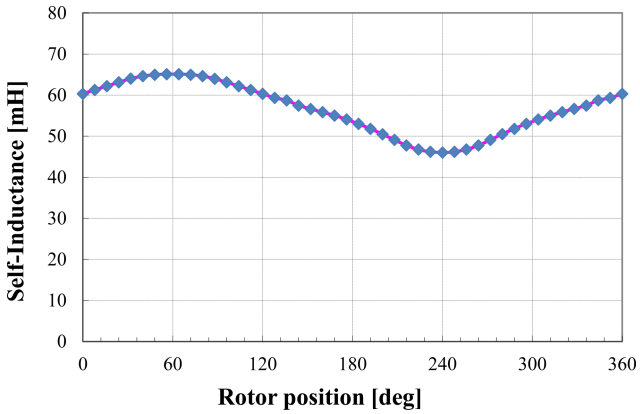

Fig. 4. (Color online) Self-inductance waveform according to rotor position.

3. Iron Loss Characteristics

3.1. Computation of the Eddy-Current Loss and Hysteresis Loss

The eddy current and the hysteresis losses of the core, W_{ie} and W_{ih}, can be calculated from the one periodic time variation of the magnetic fields obtained by the FEM [7-9] as follows:

$$W_{ie} = \frac{K_e D}{2\pi^2} \int_{CORE} \frac{1}{N} \sum_{k=1}^{N} \left\{ \left(\frac{B_r^{k+1} - B_r^k}{\Delta t} \right)^2 + \left(\frac{B_\theta^{k+1} - B_\theta^k}{\Delta t} \right)^2 \right\} dv \quad (1)$$

$$W_{ih} = \frac{K_h D}{T} \sum_{i=1}^{NE} \frac{\Delta V_i}{2} \times \left(\sum_{j=1}^{Npr^i} \left(B_{mr}^{ij} \right)^2 + \sum_{j=1}^{Np\theta^i} \left(B_{m\theta}^{ij} \right)^2 \right) \quad (2)$$

Where K_e and K_h are the eddy-current and hysteresis loss coefficient obtained by the Epstein Method. D is the density of the core, N is the number of time steps per time period, Δt is the time interval, ΔV_i is the volume of the ith finite element, B_r, B_θ are the radial and the peripheral components of the flux density, and B_{mr}^{ij}, $B_{m\theta}^{ij}$ are the

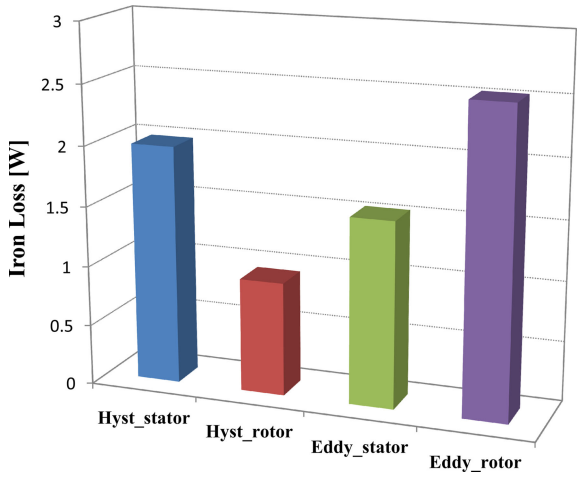

Fig. 5. (Color online) Iron losses at rated load.

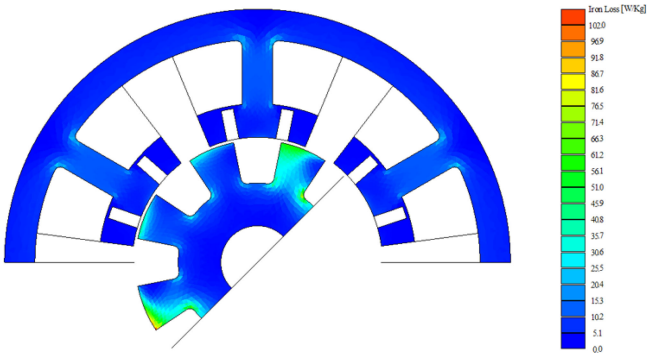

Fig. 6. (Color online) Iron loss density distribution at rated load.

amplitude of each hysteresis loop.

3.2. Analysis Results and Discussions

Fig. 5 shows the simulated iron losses of the ITFRM by the 2D-FEM at rated load. Despite the amount of the used iron in the rotor is smaller than the stator, the total iron losses of the rotor is similar to that of the stator. This is mainly due to the large variation of magnetic flux density in the rotor teeth part. The eddy current loss increases the iron loss of the rotor. The magnetic field variation in the stator teeth and yoke part is primarily due to the rotation of the magnetized rotor. Fig. 6 illustrates an iron loss density distribution. From this figure, we can also see that the density value is very large in the rotor teeth. Fig. 7 shows the variation contour of the magnetic flux density on the teeth of the stator and rotor. The stator core has an alternating magnetic field, as compared with the rotor core which has a rotating magnetic field. Generally, a rotating magnetic field generates larger iron losses. Fig. 8 compares the total iron losses according to the output of the FRM. It

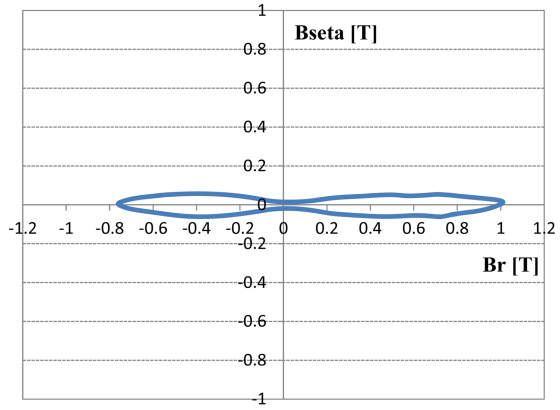

(a) Stator

(b) Rotor

Fig. 7. (Color online) Flux density contour.

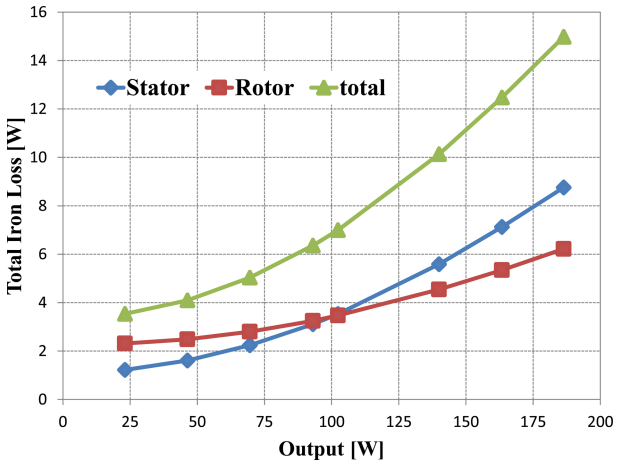

Fig. 8. (Color online) Total iron losses according to output.

shows that the total iron losses are nearly exponential. The hysteresis losses of the stator become larger than that of the rotor as the output increases. That is why the iron losses of the stator is large above 100W.

4. Irreversible Demagnetization Characteristics

4.1. The Demagnetization Analysis of a Permanent Magnet

For the irreversible demagnetization calculation of the permanent magnet, we have used an approximate equation for magnetization M of a magnet. Fig. 9 shows a typical demagnetization curve of permanent magnet materials. When operating point P1 moves to P2 because of a large external magnetic field, the residual flux density Br is decreased to B'r, and an irreversible demagnetization occurs. As a result, the magnetization M of the magnet is also decreased [10, 11].

4.2. Analysis Results and Discussions

Fig. 10 shows the magnetization distribution in the magnet according to magneto-motive force (MMF). The magnetization of the magnets lower as the MMF increases. Fig. 11 shows the generated BEMF after demagnetization. From this figure, we can see that the BEMF considerably decreases. Thus, it deteriorates the performances of the FRM such as the torque ability and efficiency. Fig. 12 illustrates the magnetization distribution according to the

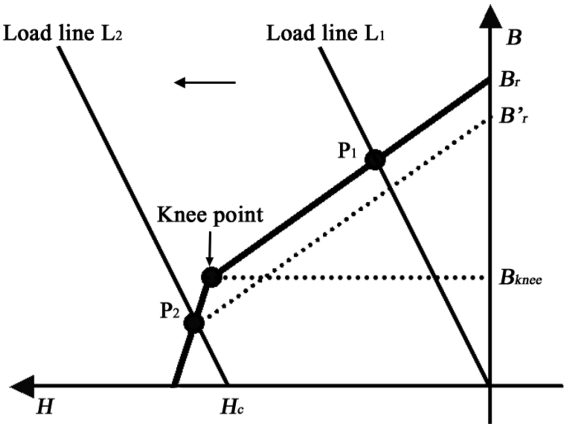

Fig. 9. Demagnetization curve of a permanent magnet.

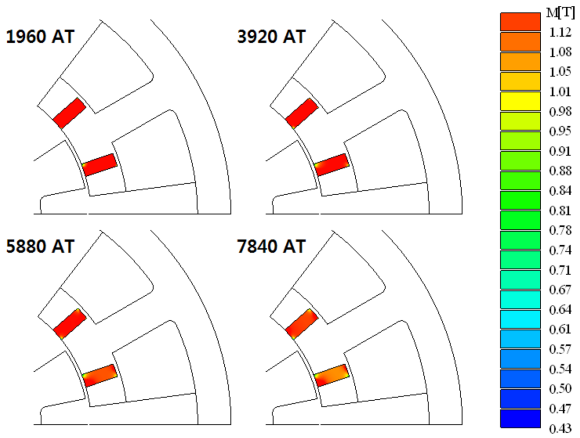

Fig. 10. (Color online) Magnetization distribution according to MMF.

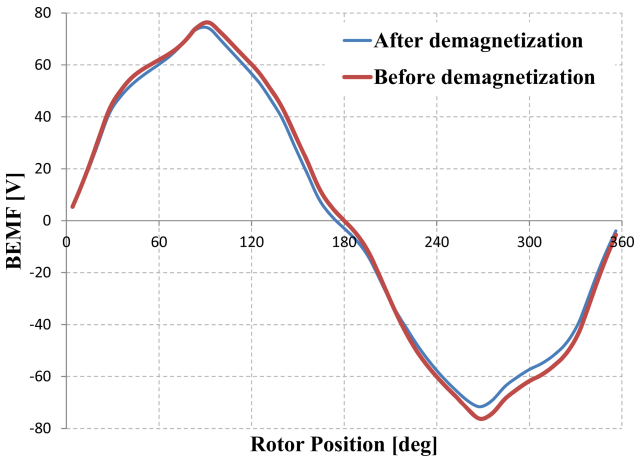

Fig. 11. (Color online) Comparison of the generated BFEM at 1500 rpm.

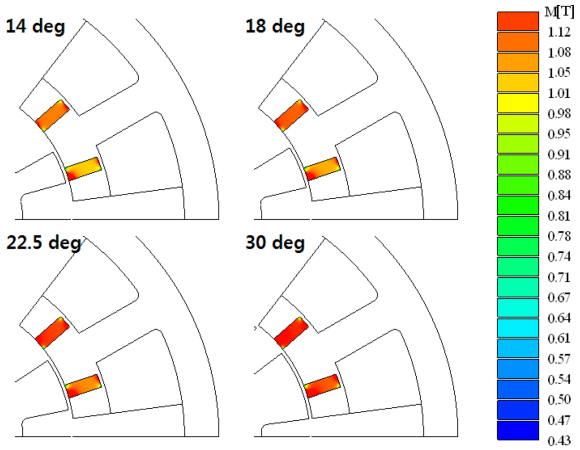

Fig. 12. (Color online) Magnetization distribution according to rotor teeth width.

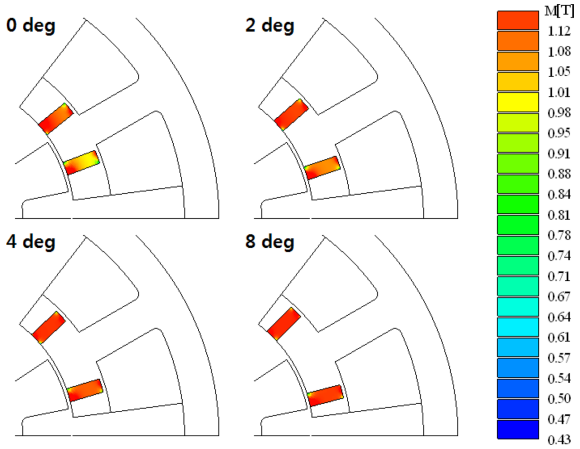

Fig. 13. (Color online) Magnetization distribution according to magnet position.

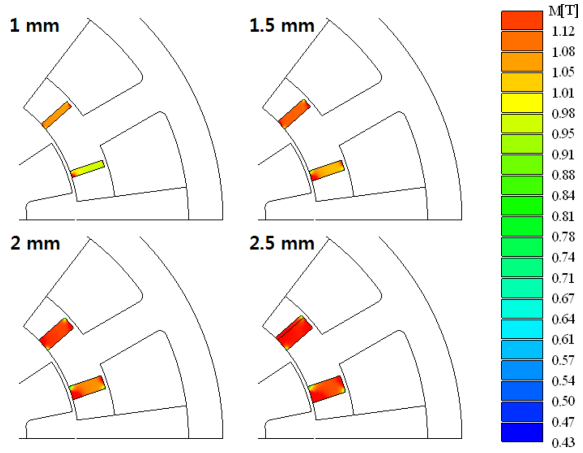

Fig. 14. (Color online) Magnetization distribution according to magnet thickness.

rotor teeth width. The more the rotor teeth width increases, the more the magnet demagnetization decreases. This is because the large MMF concentrates on the magnets through the narrow teeth width. The magnetization distribution according to the magnet position is shown in Fig. 13. The magnet placed near the edge of the stator teeth has a merit in the view of the irreversible demagnetization. This is due to the fact that the part of the magnet facing the rotor teeth is small. However, these situations are varied as the rotor rotates. The effect of the magnet thickness on the demagnetization is illustrated in Fig. 14. The magnet thickness is the most important design variable in the respect of demagnetization and efficiency.

5. Conclusions

Decreasing iron losses and avoiding the irreversible demagnetization are very important when designing the ITFRM with a high efficiency and reliability. Accordingly, their accurate simulations and evaluations are needed.

In this paper, we have analyzed the iron losses and the irreversible demagnetization characteristics of the ITFRM. The various design variables have been investigated in terms of such characteristics. To obtain an accurate analysis, we have used a 2-D finite element method with the nonlinear permanent magnet modeling. From analysis results, we can deduce that the rotor teeth part has a considerable eddy current loss and that the magnet thickness and rotor teeth width and effective design variables in terms of the irreversible demagnetization are the most important. These assumptions could be adopted to design the ITFRM with a good performance.

References

[1] Y. Liao, F. Liang, and T. A. Lipo, IEEE Trans. Ind. Appl. **31**, 1069 (1995).
[2] R. Deodhar, S. Andersson, I. Boldea, and T. J. E. Miller, IEEE Trans. Ind. Appl. **33**, 925 (1997).
[3] H. K. Shin and T. H. Kim, ICEMS, F20100713-72 (2010).
[4] H. K. Shin, T. H. Kim, and C. J. Kim, ICEMS, DS3G3-2 (2012).
[5] T. H. Kim and J. Lee, IEEE Trans. Magn. **40**, 2053 (2004).
[6] T. H. Kim, IEEE Trans. Magn. **45**, 2859 (2009).
[7] K. Yamazaki, IEEE Trans. Magn. **39**, 1460 (2003).
[8] K. Yamazaki and Y. Haruishi, IEEE Trans. Ind. Appl. **40**, 543 (2004).
[9] T. H. Kim, IEEE Trans. Magn. **43**, 1725 (2007).
[10] G. H. Kang, J. Hur, H. Nam, J. P. Hong, and G. T. Kim, IEEE Trans. Magn. **39**, 1488 (1999).
[11] J. W. Jung and T. H. Kim, J. Magnetics **15**, 40 (2010).